



HAL
open science

Mixing V2V- and non-V2V-equipped vehicles in car following

Francisco Navas, Vicente Milanés

► **To cite this version:**

Francisco Navas, Vicente Milanés. Mixing V2V- and non-V2V-equipped vehicles in car following. *Transportation research. Part C, Emerging technologies*, 2019, 108, pp.167-181. 10.1016/j.trc.2019.08.021 . hal-02392487

HAL Id: hal-02392487

<https://inria.hal.science/hal-02392487>

Submitted on 4 Dec 2019

HAL is a multi-disciplinary open access archive for the deposit and dissemination of scientific research documents, whether they are published or not. The documents may come from teaching and research institutions in France or abroad, or from public or private research centers.

L'archive ouverte pluridisciplinaire **HAL**, est destinée au dépôt et à la diffusion de documents scientifiques de niveau recherche, publiés ou non, émanant des établissements d'enseignement et de recherche français ou étrangers, des laboratoires publics ou privés.

Mixing V2V- and non-V2V-equipped vehicles in car following

Francisco Navas and Vicente Milanés.

Abstract—Cooperative Adaptive Cruise Control (CACC) provides significant traffic flow improvements when a vehicle-to-vehicle (V2V) communication link exists with the preceding vehicle, but it degrades to an Adaptive Cruise Control (ACC) when this communication link is no longer available. This degradation occurs even if the information from another V2V-equipped vehicle ahead (different to the preceding one) is still available. This paper presents a novel car-following control system—Advanced Cooperative Adaptive Cruise Control (ACACC)—that benefits from the existing communication with this vehicle ahead in the string, reducing inter-vehicle gap whereas keeping string stability. The proposed control structure provides a hybrid behaviour between two CACC controllers with different time gaps according to the string position of the vehicle with the V2V communication link available. An stable hybrid behavior between both controllers is ensured through the Youla-Kucera parameterization. Simulation and real experiments show the proper behaviour of the designed control algorithm and a good performance compared to existing ACC/CACC controllers.

Index Terms—Cooperative adaptive cruise control, V2V-equipped vehicles, non-V2V-equipped vehicles, mixed traffic situations, intelligent transportation systems.

I. INTRODUCTION

Recently, the International Council on Clean Transportation has estimated that over the next two decades vehicle ownership is expected to increase 7 million only in the European Union (EU) [1]. Therefore, road transport will have to deal with these figures. Among the associated problems, drivers will find more congested roads, resulting in an enormous waste of fuel and productivity together with health problems. According to the European Commission, congestion costs are equivalent to 1% of Gross domestic product (GDP)—in other words more than the EU budget [2].

Since building new infrastructure is no longer an appropriate solution, more intelligent and efficient options result of Intelligent Transportation Systems (ITS). Specifically, related to traffic congestion, intelligent longitudinal speed control is a suitable system to improve congestion in highways, through homogeneous speed on the part of the driver and shorter intervehicle distances. Adaptive cruise controller (ACC) [3] is a commercial system already implemented in production vehicles. An ACC system can track the preceding vehicle measuring the actual distance and the ego-vehicle velocity. These inputs allow the system to maintain a selected time gap, calculating the required acceleration or deceleration to reach the desired velocity or to prevent a collision. Recently, research focuses on the cooperative version of the system, so-called cooperative ACC (CACC) [4]. Vehicle-to-vehicle

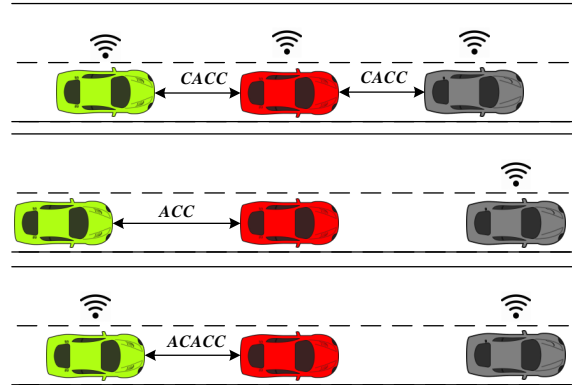


Fig. 1. ACACC scenario.

(V2V) communication is added to the existing ACC system, improving the traffic flow through the formation of a tighter string of vehicles.

Traffic flow benefits in function of the ACC-equipped vehicles market penetration have been widely studied. Kesting et Al. [5] [6] stated that a 25% of market penetration could remove congestion. Recent studies [7] proposes a different ACC model that provides no traffic flow benefits even with a market penetration of 100%. This model is based on the field test of ACC driven by 16 drivers from the general public in [8]. These drivers were encouraged to select the time gap setting that they preferred, resulting in a time-gap close to manual driving. As quantitative example, the highway capacity with every vehicle driven manually is 2050 veh/h, while with ACC-equipped vehicles the capacity increases up to 2200 veh/h [9].

In contrast, the CACC system on the traffic flow characteristics presents much more optimistic results. Arem et al. [10] conclude that CACC improves the highway capacity when the penetration rate is greater than 60%, obtaining better results on high traffic volume because of more vehicles participate in the string. The CACC model in [7] validates these results, showing a maximum lane capacity of 4000 veh/h under 100% CACC-equipped vehicles condition. This model is again based on the chosen time-gap by the general public in the field test in [8]. CACC can double the highway capacity in the ideal situation.

It is clear that the market penetration of CACC systems would progressively occur, making necessary to work with mixing traffic situations. As the highway capacity is sensitive to the percentage of CACC-equipped vehicles, it is important to preserve the CACC behaviour when there is no communication with the preceding vehicle, but with another further on the string. For instance, when a vehicle loses communication

F. Navas is with the Research Department, AKKA Technologies, France. The work was done with INRIA Paris, France. {francisco-martin.navas-matos@akka.eu}; V. Milanés is with the Research Department, Renault SAS, 1 Avenue de Golf, 78280 Guyancourt, France {vicente.milanes@renault.com}.

capability into a string previously formed by CACC-equipped vehicles. As the communication with the preceding vehicle is no longer available, existing literature on the field (see [11] and [12] for details), degrades the system to a conventional ACC, removing the strong impact of CACC systems on highway capacity. Middle plot of Fig. 1 depicts the situation. As quantitative example, [4] showed how the minimum time gap string stable increases from 0.7s to 3.16s when communication is not available.

Recent literature deals with V2V communication problem with the preceding vehicle. Van et Al. [13] used a buffer in order to store the communication with the preceding vehicle for a period of time. This buffer is combined with the vehicle model to provide robustness when intermittent communication failures occur. Savaia et Al. [14] used a Kalman filter together with the history of preceding vehicle acceleration when intermittent communication failures exist with the preceding vehicle. However, these are useful for short periods of time where communication disappears with the preceding vehicle, otherwise a degradation to ACC needs to be performed for ensuring string stability. CACC controller design when there is no communication with the preceding vehicle, but with another further on, is considered in [15]. A string of three vehicles is employed, giving guidelines in the design of a proportional-derivative (PD) controller and time gap value in order to reduce the effects of communication failures in the string stability of a CACC system. A normal CACC is considered if communication with preceding vehicle is present, otherwise the controller is switched to another one connected to the leader vehicle, avoiding system degradation to an ACC. Nevertheless, stability is not ensured when switching between both controllers, and all vehicles in the string have same dynamics and behavior.

To the best of author knowledge, former CACC working with V2V degradation study either the minimum time gap to guarantee stability according to the V2V lost, switch between CACC and ACC when the V2V link is lost [11] [12], use prediction for short period of V2V degradation [13] [14], or give control guidelines (and use communication with a vehicle further on the string) to be able to perform in a mode close to CACC for a longer period of time of degradation, but with all vehicles behaving as CACC [15]. This paper proposes a novel solution when the V2V link with the preceding vehicles is lost without degrading vehicle performance to an ACC. Different preceding vehicle behaviors are considered, it could be either as a CACC-equipped, ACC-equipped or a conventional vehicle. The principle relies on the effect that V2V info from any vehicle ahead is still available so the vehicle can be able to perform in between CACC and ACC responses, leading to shorter inter-vehicular gaps whereas keeping string stability. Besides, Youla-Kucera (YK) parameterization is used in order to ensure stability when adapting the control response between both controllers.

The control algorithm proposed in this work—Advanced CACC (ACACC)—benefits from the V2V information coming from another vehicle ahead in the string instead of degrading to a conventional ACC when there is no communication with the preceding vehicle. Preceding vehicle behavior could be

either as a CACC-equipped, ACC-equipped or a conventional vehicle. Since the time gap policy has a significant influence on the highway capacity, ACACC is specifically composed by two CACC controllers with different time gaps. An hybrid behavior between both could not be stable. In [16], a theoretical example shows how the linear combination of two stabilizing controllers does not result in a stabilizing controller of the system. Different controller interpolation methods have been proposed in the literature to guarantee stability. [17] proposed an algorithm for linear interpolation based on eigenplacement of state feedback gains. In [18] and [19], approaches for interpolation based on coprime factors and state-space representation are presented. [20] used the YK parameterization of all the controllers to provide controllers' interpolation with guaranteed stability. Later, [21] and [22] guaranteed stability under arbitrary change of the signal responsible of the interpolation over time. Several practical applications of YK parameterization can be found in the project called Plug&Play [23]. YK is chosen among the others to obtain a stable interpolation between the two CACC controllers that compose the proposed ACACC system.

Traffic flow improvement comes from a hybrid behaviour between both while using the existing communication link with the closer ahead communicated vehicle. As the system is not degraded to ACC, the highway capacity previously accomplished by the CACC string of vehicles is better preserved, as well as the shockwave effect is better mitigated. The bottom part of Fig. 1 shows an ACACC scenario; where the red vehicle could be either a conventional driver or an ACC-equipped vehicle, both without communication capabilities.

The proposed system has been simulated for highway velocities by using the vehicle model in [24]. ACACC has been tested under different situations, being the preceding vehicle either a conventional or an ACC-equipped one. For all cases, the system exhibits a good performance, achieving a tighter string of vehicles. These simulations results are later validated on the INRIA experimental platform at low-speeds. ACACC improves traffic flow capacity.

In brief, the main contributions in this paper are the following:

- ACACC benefits for any V2V-equipped vehicle ahead when communication with the preceding one is lost, avoiding a full ACC degradation. Communication unavailability could be either intermittent or permanent.
- ACACC is composed by two CACC controllers with different time gaps. YK parameterization is used with these two controllers in order to guarantee a stable interpolation between both.
- Scalar factor γ , in charge of interpolation between two controllers in a YK approach, is designed in order to improve traffic flow (reduce inter-vehicle distance, while being string stable).
- The approach is adaptable for any type/number of preceding vehicles. Simulation results are provided, being the preceding vehicle either a conventional vehicle emulated by an Intelligent Driver Model (IDM), an ACC-equipped one, or even several ACC-equipped vehicles; all of them

without communication capabilities. Simulations results are validated at INRIAs low-speed experimental platform.

The rest of the paper is structured as follows. Section II introduces the problem formulation, including the basis of a CACC control algorithm and some initial assumptions. The theory for ensuring a stable interpolation between two general controllers is described in Section III. How this theory is applied to ACACC scenario and how the percentage of each CACC controller is modified through γ for improving highway capacity is presented in Section IV. Section V shows simulation results. The control algorithm is validated on the low-velocity experimental platform in Section VI. Finally, some concluding remarks are given.

II. PROBLEM FORMULATION

A string of n vehicles driving in the same lane, one after the other, is considered. i determines the order of a vehicle inside of the string $i \in [1, n]$. Vehicle 1 is the leader and first vehicle in the string, vehicle i denotes ego-vehicle and vehicle $i-1$ is the vehicle preceding the ego-vehicle. Leader and preceding vehicle are the same vehicle when $n=2$. If $n \geq 3$, the number of vehicle between leader 1 and ego vehicle i is $n-2$. Problem formulation focuses on ego-vehicle situation according to V2V communication availability with vehicle $i-1$ and the rest of vehicles in the string. V2V communication between vehicle i and vehicle $i-1$ is defined as C_{i-1} . Communication between vehicle i and some other vehicle x different from the preceding one is defined as C_x with $1 \leq x < i-1$.

In the literature, communication availability with vehicle $i-1$ determines the use of ACC or CACC controllers in the vehicle i , and therefore its time gap policy h_i :

- When C_{i-1} exists, a regular CACC controller can be used. Faster responses can be achieved, allowing a tighter string of vehicles by employing a time gap h_{CACC} —i.e. $\exists C_{i-1} \rightarrow CACC$ where $h_i = h_{CACC}$.
- If C_{i-1} is no longer available: the system degrades to a conventional ACC algorithm [25]. Consequently, benefits of CACC systems on highway capacity are removed because a longer time gap $h_{ACC} > h_{CACC}$ needs to be set to ensure string stability—i.e. $\nexists C_{i-1} \rightarrow ACC$ where $h_i = h_{ACC} > h_{CACC}$.

These situations have been extensively studied (see [3] for ACC and [4] for CACC for details), but potential benefits of using C_x when C_{i-1} is not available have not been further investigated. Speed oscillations on the string (i.e. the difference between speeds V_x and v_{i-1}) is limited to 5m/s according to [11]. Experimental results demonstrated that over this value, drivers disengage ACC system due to its degraded performance.

The objective of the ACACC controller is to enhance traffic flow when there is no communication with vehicle $i-1$ (preceding vehicle), by taking the information from the closer V2V-equipped vehicle ahead, in that case, vehicle x (that could be either the leader vehicle or another one between preceding and leader). Since V2V communication is always available (no matter from which vehicle comes from), a CACC control structure is proposed (see Sec. II.A for details). ACACC is

composed by two CACC controllers with different time gaps: A CACC controller with a short time gap $h_i = h_{CACC}$ so-called $CACC_{STG}$ when C_{i-1} is available; and a CACC controller with a longer time gap $h_i = h_{ACC}$ so-called $CACC_{LTG}$ when C_{i-1} is lost but C_x link is still available. The proposed ACACC algorithm benefits from the YK parameterization to provide a hybrid response between both controllers, assuring control system stability. The regulation between the effect of each controller in the control command is based on a correlation between the speed received via V2V communication and the one detected by the on-board ego-vehicle sensor (i.e. radar). The correct tuning of γ with a maximum speed oscillation of 5m/s, assures string stability and improves traffic flow.

In brief, ACACC works when C_{i-1} is lost but C_x is available, providing a control structure of the form:

$$ACACC = CACC_{STG}(1 - \gamma) + CACC_{LTG}\gamma; \quad \gamma \in [0, 1] \quad (1)$$

where $h_i \in [h_{CACC}, h_{ACC}]$. Notice how the time gap would be lower than degrading the system to a regular ACC.

A. CACC

Figure 2 shows the classical structure for CACC systems (see [4] for more details), where G represents the vehicle model, K_i a stabilizing controller and V_{i-1}^c the control velocity of vehicle $i-1$ communicated through C_{i-1} by means of a feedforward filter F_i . The controller should be able to regulate the error e_i between relative distance $d_{r,i}$ ($X_{i-1} - X_i$, as difference between absolute positions) and the reference distance coming from the spacing policy ($V_i h_i$, where V_i is the ego-vehicle velocity). In previous study [26], PD controller has provided good performance. PD controller expression is in equation (2). Controller parameters $k_{p,i}$ and $k_{d,i}$ will change for $CACC_{STG}$ and $CACC_{LTG}$ in the proposed ACACC approach,

$$K_i = k_{p,i} + k_{d,i}s \quad (2)$$

Highway capacity improves when tighter gap policies can be adopted whereas keeping string stability. String stability is defined as the attenuation of disturbances along the string of vehicles. A sufficient condition for string stability is given in [27], which means that the absolute position of each vehicle must not increase as it propagates through the string. Condition is equivalent to equation (3).

$$\|X_i/X_{i-1}\|_\infty \leq 1 \quad \text{for } i > 1 \quad (3)$$

According to [26], for a PD-based CACC system the string stability function results:

$$\frac{X_i}{X_{i-1}} = \frac{D_i + (1 + h_i s)GK_i}{(1 + h_i s)(1 + (1 + h_i s)GK_i)}, \quad \text{for } i > 1 \quad (4)$$

Under the ideal situation where the communication delay is null ($D_i = 1$), string stability yields:

$$\frac{X_i}{X_{i-1}} = \frac{1}{(1 + h_i s)}, \quad \text{for } i > 1 \quad (5)$$

Therefore, string stability is guaranteed for any $h_i > 0$. The existence of C_{i-1} makes vehicle response faster, allowing any

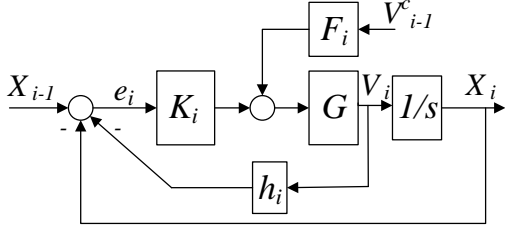


Fig. 2. Classical CACC control structure.

time gaps without compromising the string stability. On the contrary, as the ACC system has not C_{i-1} , the achievable stable time gap is longer, even close to the time gap of a manual driver. It explains why even with a high market penetration of ACC-equipped vehicles the traffic flow improvement effects are not visible.

B. Initial assumptions

The next assumptions have been considered in the analysis:

- Ego-vehicle (vehicle i) is at least the third vehicle in the string, meaning that there is a preceding one (vehicle $i-1$) whose V2V link is lost and a vehicle x (that could be the leader ($x=1$), or some other if $n > 3$) broadcasting its information.
- Maximum string length is limited to the speed difference value that makes drivers disengage ACC systems. Milanés et Al. [24] shows that this difference is equal to $5m/s$ and this value is reached in a six ACC-equipped vehicles string. V2V studies using Dedicated Short Range Communication (DSRC) guarantees up to 300m [28], which also matches with the six-vehicles string assumption to guarantee communication even between leading and the last vehicle in the string.
- The communicating vehicle ahead is in the same lane. This can be known from a digital map and can be part of the transmitted information.
- Communication link between vehicles is considered ideal. No delay is present in the communication system.

III. YOULA-KUCERA CONTROLLER MODIFICATION

This section introduces the mathematical basis in which YK relies on to ensure stable interpolation between different controllers. The change between both controllers is made through the parameterization of all the controllers that stabilizes a given plant [29]. At the same time, the parameterization is based on the doubly coprime factorization [30].

The notation is standard; $\mathbb{RH}_\infty^{p \times m}$ is the real stable transfer function space which maps m -dimensional inputs into p -dimensional outputs.

$$y = Gu, \quad y \in \mathbb{R}^p \quad \text{and} \quad u \in \mathbb{R}^m \quad (6)$$

where G is the plant; y the measurement vector corresponding to the output and u the control signal. The dimension of both signals is $p = m = 1$.

The plant could be stabilized by any appropriate LTI controller K_i . Assuming that K_0 corresponds to $CACC_{STG}$ and K_1 to $CACC_{LTG}$, it will be possible to do a stable interpolation between them thanks to the YK parameterization of all controllers.

The plant G and both controllers K_0 and K_1 need to be factorized to apply YK theory.

A. Doubly coprime factorization

Double coprimeness refers to the idea of being right and left coprime [31].

Definition 1: Two different matrices M and N are right coprimes over $\mathbb{RH}_\infty^{p \times m}$ if they have the same number of columns and if matrices X_r and Y_r exist such that:

$$\begin{bmatrix} X_r & Y_r \end{bmatrix} \begin{bmatrix} M \\ N \end{bmatrix} = X_r M + Y_r N = I \quad (7)$$

Definition 2: Two different matrices \tilde{M} and \tilde{N} are left coprimes over $\mathbb{RH}_\infty^{p \times m}$ if they have the same number of rows and if matrices X_l and Y_l exist such that:

$$\begin{bmatrix} \tilde{M} & \tilde{N} \end{bmatrix} \begin{bmatrix} X_l \\ Y_l \end{bmatrix} = \tilde{M} X_l + \tilde{N} Y_l = I \quad (8)$$

These coprime factorizations should be such that G and K_i are:

$$\begin{aligned} G &= NM^{-1} = \tilde{M}^{-1} \tilde{N} \\ K_i &= U_i V_i^{-1} = \tilde{V}_i^{-1} \tilde{U}_i \end{aligned} \quad (9)$$

At the same time, these coprime factorizations $U_i \in \mathbb{RH}_\infty^{m \times p}$, $\tilde{U}_i \in \mathbb{RH}_\infty^{m \times p}$, $V_i \in \mathbb{RH}_\infty^{p \times p}$, $\tilde{V}_i \in \mathbb{RH}_\infty^{p \times p}$, $N \in \mathbb{RH}_\infty^{p \times m}$, $\tilde{N} \in \mathbb{RH}_\infty^{p \times m}$, $M \in \mathbb{RH}_\infty^{p \times m}$ and $\tilde{M} \in \mathbb{RH}_\infty^{p \times m}$ satisfy the double Bézout's identity [32].

$$\begin{bmatrix} \tilde{V}_i & -\tilde{U}_i \\ -\tilde{N} & \tilde{M} \end{bmatrix} \begin{bmatrix} M & U_i \\ N & V_i \end{bmatrix} = \begin{bmatrix} M & U_i \\ N & V_i \end{bmatrix} \begin{bmatrix} \tilde{V}_i & -\tilde{U}_i \\ -\tilde{N} & \tilde{M} \end{bmatrix} = \begin{bmatrix} I & 0 \\ 0 & I \end{bmatrix} \quad (10)$$

Coprime factorization related to any stabilizing controller in state space can be obtained if the theorem shown below is fulfilled [33]. Otherwise, the search of these factors could become complex.

Theorem 1: Consider a plant in state space representation as $G(s) = C(sI - A)^{-1}B$ with A, B, C stabilizable and detectable and a stabilizing controller $K_i(s) = C_{k,i}(sI - A_{k,i})^{-1}B_{k,i} + D_{k,i}$. F and $F_{k,i}$ should be chosen such that $A + BF$ and $A_{k,i} + B_{k,i}F_{k,i} \in \mathbb{RH}_\infty^{p \times m}$. Then the matrices given by

$$\begin{bmatrix} M & U_i \\ N & V_i \end{bmatrix} = \left[\begin{array}{cc|cc} A + BF & 0 & -B & 0 \\ 0 & A_{k,i} + B_{k,i}F_{k,i} & 0 & B_{k,i} \\ -F & C_{k,i} + D_{k,i}F_{k,i} & I & D_{k,i} \\ -C & F_{k,i} & 0 & I \end{array} \right] \quad (11)$$

$$\begin{bmatrix} \tilde{V}_i & -\tilde{U}_i \\ -\tilde{N} & \tilde{M} \end{bmatrix} = \left[\begin{array}{cc|cc} A + BD_{k,i}C & BC_{k,i} & -B & BD_{k,i} \\ B_{k,i}C & A_{k,i} & 0 & B_{k,i} \\ F - D_{k,i}C & -C_{k,i} & I & -D_{k,i} \\ C & -F_{k,i} & 0 & I \end{array} \right] \quad (12)$$

satisfy (9) and (10).

Notice how M and N remain the same for the plant G , as uncertainties are not taken into account in the model; while U_0 and V_0 will change to U_1 and V_1 when switching from the initial controller K_0 to the final one K_1 .

B. YK parameterization of all stabilizing controllers

YK parameterization provides all stabilizing controllers for a given plant G by interconnecting an initial controller with a parameter Q , called YK parameter, which can be any stable system with appropriate dimensions:

$$K = (U_0 + M\gamma Q)(V_0 + N\gamma Q)^{-1} = (\tilde{V}_0 + \gamma Q\tilde{N})^{-1}(\tilde{U}_0 + \gamma Q\tilde{M}), \quad Q \in \mathbb{RH}_\infty^{p \times m} \quad (13)$$

From the general description of any stabilizing controller in equation (13), it is possible to do interpolation between controllers K_0 to K_1 online, without losing stability. To preserve a good transition between both controllers, the parameter Q should be regulated by a scalar factor $\gamma \in [0, 1]$. Mixed behaviours between both controllers can be obtained by applying different values of γ . But first, the value of Q should be obtained as follows (for further details [20]):

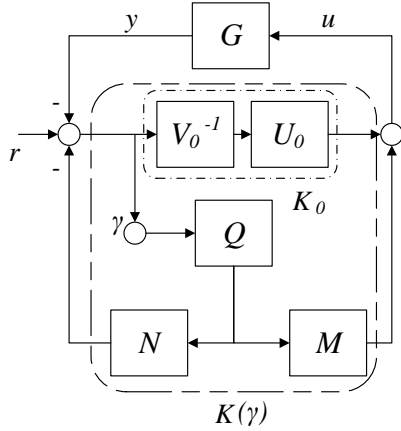


Fig. 3. Control structure for modifying controllers online.

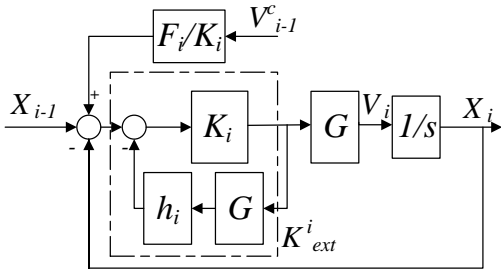


Fig. 4. Modified CACC control structure.

Theorem 2: Let NM^{-1} be a coprime factorization of the model G and $K_0 = U_0V_0^{-1} = \tilde{V}_0^{-1}\tilde{U}_0$ a stabilizing controller. A second controller is given $K_1 = U_1V_1^{-1} = \tilde{V}_1^{-1}\tilde{U}_1$. If

$$G * K_1 \in \mathbb{RH}_\infty \wedge \tilde{V}_1\tilde{V}_0^{-1}V_1 \in \mathbb{RH}_\infty \quad (14)$$

It is equivalent to the existence of Q , so all the stabilizing controllers are described by:

$$K_1 = (V_0 + Q\tilde{N})^{-1}(U_0 + Q\tilde{M}) \quad (15)$$

where Q can be calculated as:

$$Q = \tilde{U}_1 - \tilde{V}_1\tilde{V}_0^{-1}\tilde{U}_0 \quad (16)$$

This theorem allows obtaining a control structure able to do stable interpolation between different controllers. Theorem 2 is used for getting the control structure shown in Fig. 3.

When doing controller interpolation, γ plays a key role. It regulates the different levels of activation of the YK parameter Q . γ may vary from 0 to 1, being 0 a 100% contribution of K_0 and 1 a 100% contribution of K_1 .

The stability in the transition is ensured when $Q \in \mathbb{RH}_\infty$; so any linear combination of Q and γ will provide stable responses [20].

TABLE I
CACC PARAMETERS.

	K_{ext}^i	$k_{p,i}$	$k_{d,i}$	h_i
$CACC_{STG}$	K_{ext}^0	$k_{p,0}$	$k_{d,0}$	$h_0 = h_{CACC} = 0.6s$
$CACC_{LTG}$	K_{ext}^1	$k_{p,1}$	$k_{d,1}$	$h_1 = h_{ACC} = 1.5s$

IV. ACACC

ACACC is composed by two different CACC controllers: $CACC_{STG}$ and $CACC_{LTG}$. Time gap values h_{CACC} and h_{ACC} are chosen according to the general public accepted time gaps for CACC and ACC systems [8]. For CACC, the shortest gap is set at 0.6s, while for ACC is set to 1.5s.

For each of these controllers, the PD-based CACC controller seen in Fig. 2 is reformulated in Sec. IV.A to include the time gap h_i into the controller. This modification of the classical structure allows stable interpolation between controllers with different h_i , $k_{p,i}$ and $k_{d,i}$. By taking the general theory in Sec. III a control structure for making stable transitions between $CACC_{STG}$ and $CACC_{LTG}$ is shown in Sec. IV.B.

Once the control structure is obtained, a different percentage of each of the controllers is applied depending on the traffic situation. The percentage is chosen through the YK gamma γ .

The algorithm for discriminating if the information received via V2V is coming either from vehicle $i-1$ or from vehicle x in the string is out of the scope of this paper (see [34] for a possible implementation).

In Sec. IV.C, γ is designed to be modified depending on the communicated velocity V_x and the velocity of the preceding vehicle received through the onboard sensor system V_{i-1}^s .

A. Modification of classical CACC structure

The classical PD-based CACC controller is modified in Fig. 4 to include the time gap h_i into the controller. In that way, it will be possible to change the time gap of the system when doing controllers interpolation. The extended controller K_{ext}^i results in the transfer function (17). The feedforward filter is changed to F_i/K_i .

$CACC_{STG}$ has the index $i = 0$, while $CACC_{LTG}$ has the index $i = 1$. The information related to both controllers is summarized in Table I. Notice how the values of $k_{p,0}$, $k_{p,1}$, $k_{d,0}$ and $k_{d,1}$ will depend on the accepted time gaps by drivers and the vehicle model G .

$$K_{ext}^i(s) = \frac{K_i}{1 + Gh_i K_i} = \frac{k_{p,i} + k_{d,i}s}{1 + Gh_i(k_{p,i} + k_{d,i}s)} \quad (17)$$

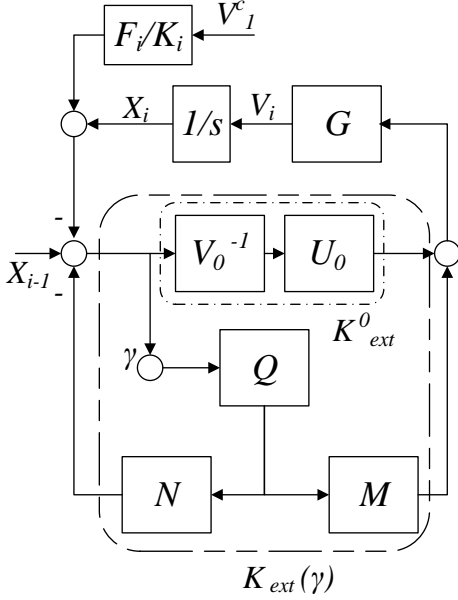


Fig. 5. YK control structure for modifying CACC controllers online.

B. Control structure for CACC controller modification

Once $CACC_{STG}$ and $CACC_{LTG}$ are defined, is possible to have hybrid behaviours between both, without losing stability by obtaining the parameter Q with Theorem 2. Figure 5 modifies the control structure in Fig. 3 to allow CACC controller modification. Please notice how the structure only differs in adding the filtered communication link with the closest V2V-equipped vehicle, in that case, communication link C_x .

C. YK gamma tuning

Once the YK control structure for CACC is obtained, a different percentage of each of the controllers is applied depending on the traffic situation. $\gamma = 0$ when C_{i-1} exists, while a simple decision-making system is used when C_{i-1} does not exist, but there is communication with a vehicle x , C_x . Gamma tuning is chosen in order to improve traffic flow:

$$\gamma = \begin{cases} 0.033(V_{i-1}^s - V_x) + 0.5 & \text{if } |V_x - V_{i-1}^s| < 5m/s \& \exists C_x \& \nexists C_{i-1} \\ 0 & \text{if } \exists C_{i-1} \end{cases}$$

where V_{i-1}^s is the velocity of the vehicle $i-1$ obtained through the on-board sensor systems, and V_x is the velocity of vehicle x received through C_x . A maximum speed oscillation of $5m/s$ is considered as the operation range for the present application.

Different traffic situations are pictured for understanding the tuning of γ when $\nexists C_{i-1}$. When vehicle $i-1$ has a behaviour similar to vehicle x , γ is modified to response faster to speed changes:

- If vehicle x accelerates, V_x will be higher than V_{i-1}^s . So, γ decreases, making the gap time shorter.
- If vehicle x brakes, V_x will be lower than V_{i-1}^s . So, γ increases, making the gap time longer.
- When both vehicle x and vehicle $i-1$ have similar velocities, γ results in an intermediate value between both controllers.

The feedforward filter F is modified accordingly to the gamma range as:

$$F' = \begin{cases} (0.033(V_{i-1}^s - V_x) + 1.0) \cdot F_0/K_0 & \text{if } |V_x - V_{i-1}^s| < 5m/s \& \exists C_x \& \nexists C_{i-1} \\ F_0/K_0 & \text{if } \exists C_{i-1} \end{cases}$$

V. SIMULATION RESULTS

This section presents the ACACC performance at high speeds (i.e. highway scenario). For simulation purposes, the vehicle model introduced in [24] is used. It is a second-order response with a time delay coming from a Nissan Infiniti M56. For the sake of clarity, vehicle transfer function is shown in (18).

$$G(s) = \frac{1.136}{s^2 + 1.067s + 1.1385} e^{-0.287s} \quad (18)$$

The algorithm performance is tested by using as vehicle $i-1$ a non V2V-equipped vehicle. It is modelled as a human driver—using the Intelligent Driver Model (IDM) [35]—or equipped with an ACC system.

A. Control system stability

$CACC_{STG}$ and $CACC_{LTG}$ controller parameters are shown in Table II. Control system stability for the designed ACACC is studied in function of γ . A necessary and sufficient condition to ensure control system stability for a feedback/feedforward control loop as the one in Fig. 5 is:

$$\begin{aligned} & \begin{bmatrix} I & -K_{ext}(\gamma) \\ -G/s & I \end{bmatrix}^{-1} \in \mathcal{RH}_\infty = \\ & = \frac{K_{ext}(\gamma)G/s}{1 + K_{ext}(\gamma)G/s} = \frac{\frac{K_{ext}^0 + M_0\gamma Q}{1 + N_0\gamma Q} G/s}{1 + \frac{K_{ext}^0 + M_0\gamma Q}{1 + N_0\gamma Q} G/s} \in \mathcal{RH}_\infty \quad (19) \\ & \text{with } F_0/K_0 \in \mathcal{RH}_\infty \end{aligned}$$

As the feedforward filter is already stable, poles of the resulting transfer function in equation (19) are analysed for different values of γ . Closed-loop (CL) poles are in Table III. CL poles during the transition are the combination of CL poles of $(G/s, K_{ext}^0)$ and $(G/s, K_{ext}^1)$. Control system stability is ensured for every value of γ .

String stability is also analysed. First, when there is communication with the preceding vehicle (see equation (3)): Fig. 6 represents the stability surface for the designed ACACC in function of the γ value. One can appreciate how the infinity norm $\|X_i/X_{i-1}\|$ is always below the unity for any value of γ , proving string stability. Second, when there is no communication with the preceding vehicle, but another further on: Control velocity V_x^c (with $x = 1$ in the case of a string

of three vehicles) is received instead of V_{i-1}^c . The designed YK gamma tuning is employed in this situation. Figure 7 considers difference between V_{i-1}^s and V_1 up to $15m/s$. As ACACC application range is up to $5m/s$, string stability is ensured even if communication with the preceding vehicles is not available.

TABLE II
NISSAN INFINITI M56 CACC PARAMETERS.

	K_{ext}^i	$k_{p,i}$	$k_{d,i}$	h_i
$CACC_{STG}$	K_{ext}^0	$k_{p,0} = 0.45$	$k_{d,0} = 0.25$	$h_0 = h_{CACC} = 0.6s$
$CACC_{LTG}$	K_{ext}^1	$k_{p,1} = 0.45$	$k_{d,1} = 0.25$	$h_1 = h_{ACC} = 1.5s$

TABLE III
CL POLES ($G/s, K_{ext}(\gamma)$). YK CONTROLLER RECONFIGURATION BETWEEN K_{ext}^0 AND K_{ext}^1 . NISSAN INFINITI M56.

γ	CL poles
$\gamma = 0.0$	$[-6.28e^7, 0, -0.61 \pm 1.08i]$
$\gamma = 0.1$	$[-6.28e^7, -6.28e^7, 0, 0, -0.74 \pm 1.16i, -0.61 \pm 1.03i]$
$\gamma = 0.2$	$[-6.28e^7, -6.28e^7, 0, 0, -0.74 \pm 1.16i, -0.61 \pm 1.03i]$
$\gamma = 0.3$	$[-6.28e^7, -6.28e^7, 0, 0, -0.74 \pm 1.16i, -0.61 \pm 1.03i]$
$\gamma = 0.4$	$[-6.28e^7, -6.28e^7, 0, 0, -0.74 \pm 1.16i, -0.61 \pm 1.03i]$
$\gamma = 0.5$	$[-6.28e^7, -6.28e^7, 0, 0, -0.74 \pm 1.16i, -0.61 \pm 1.03i]$
$\gamma = 0.6$	$[-6.28e^7, -6.28e^7, 0, 0, -0.74 \pm 1.16i, -0.61 \pm 1.03i]$
$\gamma = 0.7$	$[-6.28e^7, -6.28e^7, 0, 0, -0.74 \pm 1.16i, -0.61 \pm 1.03i]$
$\gamma = 0.8$	$[-6.28e^7, -6.28e^7, 0, 0, -0.74 \pm 1.16i, -0.61 \pm 1.03i]$
$\gamma = 0.9$	$[-6.28e^7, -6.28e^7, 0, 0, -0.74 \pm 1.16i, -0.61 \pm 1.03i]$
$\gamma = 1.0$	$[-6.28e^7, 0, -0.74 \pm 1.16i]$

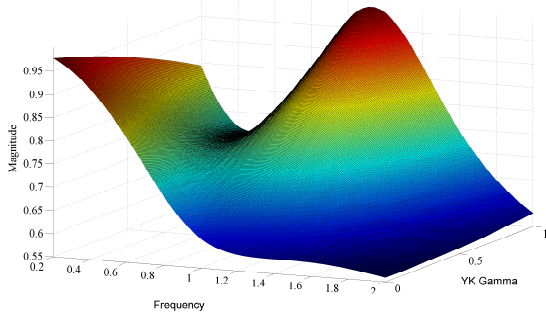


Fig. 6. String stability's surface for a Nissan Infiniti M56s depending on YK γ . Preceding vehicle's communication is available.

B. Using IDM as preceding non V2V-equipped vehicle

First simulations consider a human-driven vehicle (modelled by the IDM) as vehicle $i - 1$ without communication. IDM is a well-known car-following model in the traffic flow simulation literature [35]. It defines a target acceleration depending on desired velocity, desired time gap and comfortable deceleration. The parameters in [11] are used as reference values.

Figure 8 depicts the performance of the ACACC controller in comparison with ACC and CACC (assuming V2V capabilities in the IDM vehicle, only in the CACC case) controllers

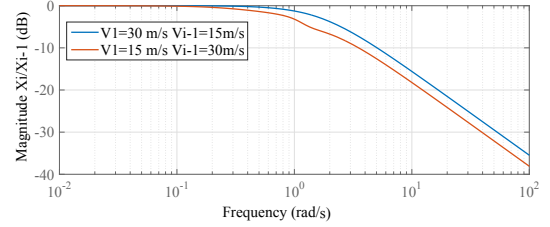


Fig. 7. String stability magnitude in dB for a Nissan Infiniti M56 when communication with preceding vehicle is not available, but it is with another vehicle further on the string. $|V_x - V_{i-1}^s| = 15m/s$.

when the IDM desired velocity is $33.33m/s$. The top graph plots the vehicles' speeds. The second graph plots the vehicles' accelerations during the simulation. The third graph shows the relative distance between vehicles. The bottom graph represents how γ is modified together with the real time gap. A string of three vehicles is considered. For notation, vehicle 1 (solid magenta line) is a V2V-equipped vehicle and the first vehicle during the whole simulation; vehicle $i - 1$ (solid cyan line) is the one that starts the platoon in the second position as IDM; and, the vehicle i or follower is either an ACC-equipped vehicle (solid red line), a CACC-equipped vehicle (solid green line, assuming that the IDM is V2V-equipped for comparison purposes) or an ACACC-equipped vehicle (solid blue line).

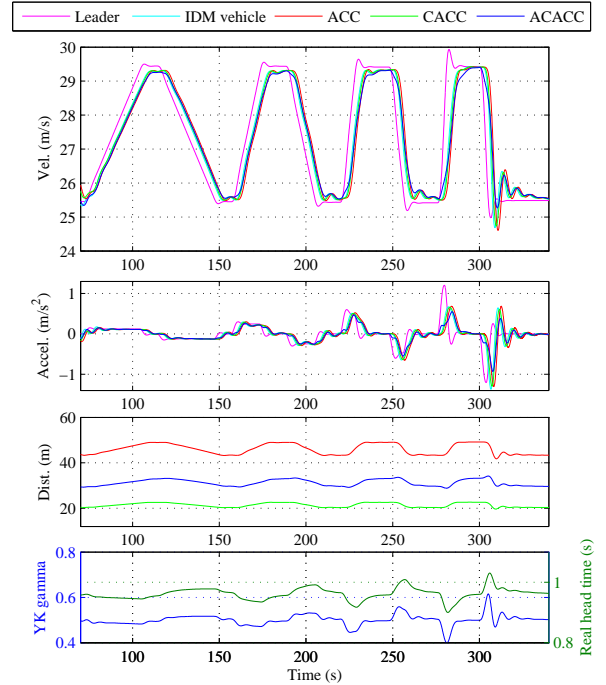


Fig. 8. Simulation results comparison among car-following policies using CACC, ACC and ACACC controllers when a non V2V-equipped vehicle is in front. The non V2V-equipped is a conventional driver emulated by a IDM with a desired velocity of $33.33m/s$.

The value of γ is always around 0.5, changing with acceleration or braking changes. The performance of the ACACC system is a hybrid response between $CACC_{STG}$ and $CACC_{LTG}$. Its response comes earlier to changes in leader speed V_x than the ACC/CACC systems. For instance, when vehicle 1 is

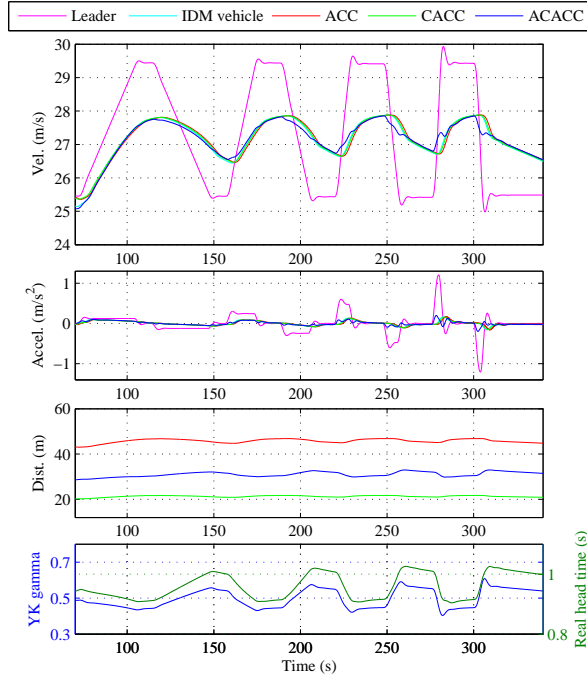


Fig. 9. Simulation results comparison among car-following policies using CACC, ACC and ACACC controllers when a non V2V-equipped vehicle is in front. The non V2V-equipped is a conventional driver emulated by an IDM with a desired velocity of $28m/s$.

braking at 300s, the ACACC system brakes practically at the same time, while ACC and CACC react 5s later. Besides, the system is more damped while speed changes take place, better preserving string stability. Finally, the main objective of the present paper is also fulfilled, instead of degrading to an ACC system, ACACC takes C_1 for making the string of vehicles tighter, improving highway capacity. The relative distance corresponds to a spacing policy between $CACC_{STG}$ and $CACC_{LTG}$ responses.

Figure 9 shows a second simulation using IDM. The desired velocity parameter from [11] is change from $33.33m/s$ to $28m/s$, emulating a very slow vehicle dynamic on the non V2V-equipped vehicle $i-1$ when tracking changes in V_x . Since the IDM model is not correctly following vehicle 1 response, the ACACC system has a closer behaviour to $CACC_{LTG}$. This behaviour is appreciated on the lower plot of Fig. 9.

C. Using an ACC-equipped vehicle as preceding non V2V-equipped one

Milanés and Shladover [11] compare the car following performance among ACC and CACC systems for a Nissan Infiniti M56s. Experimental results are used to obtain car-following models for representing the production ACC and the new designed CACC controller, highlighting how the production ACC results string unstable, amplifying the speed changes of the preceding vehicle. A simulation using the ACC/CACC car-following models presented in [11] is carried out. Specifically, the more the ACC-equipped vehicles in the string, the bigger the amplification. Here, instead of degrading

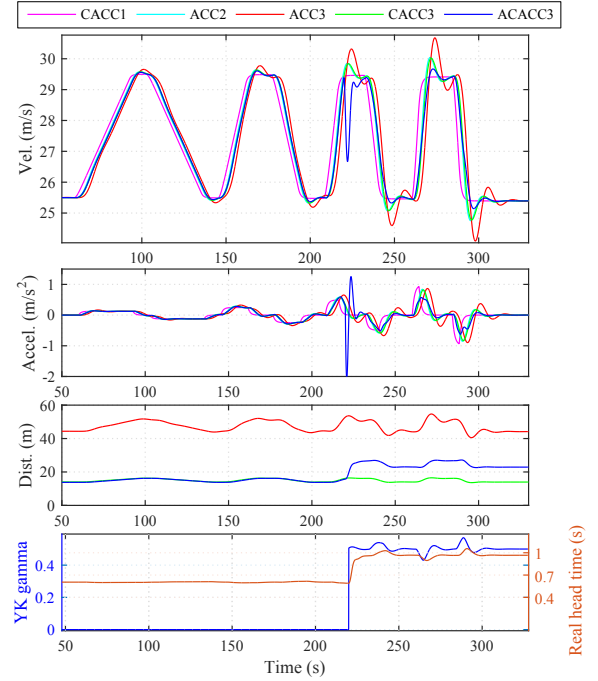


Fig. 10. Simulation results comparison among car-following policies using CACC, ACC and ACACC controllers when communication is lost with a V2V-equipped vehicle. Preceding vehicle is an ACC-equipped vehicle with communication capabilities. Communication is lost at 220s.

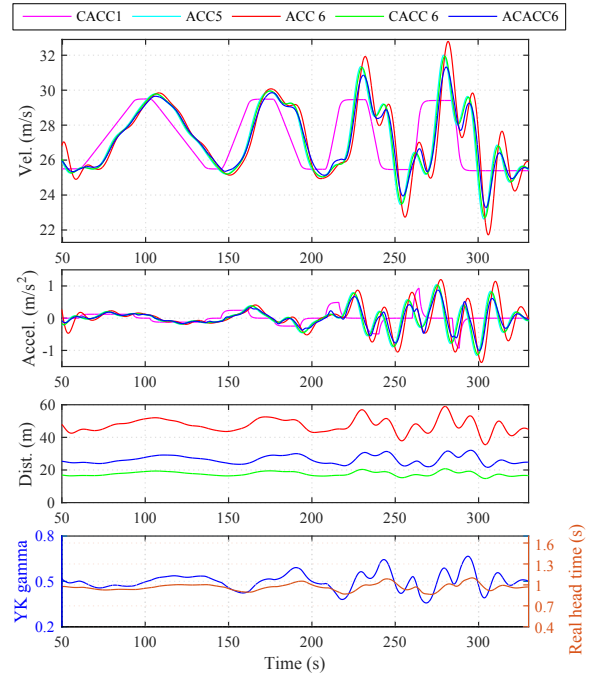


Fig. 11. Simulation results comparison among car-following policies using CACC, ACC and ACACC controllers when four non V2V-equipped vehicle are in front. The non V2V-equipped are ACC-equipped vehicles. Communication is available with the first vehicle of the string, CACC-equipped.

the system to another ACC, the system is changed to ACACC with C_1 .

Figure 10 depicts the performance of the ACACC controller in comparison with ACC and CACC controllers when an ACC-

equipped vehicle is the vehicle $i-1$. Vehicle $i-1$ is a V2V-equipped vehicle that loses its communication capability at 220s. A string of three vehicles is considered. For notation, vehicle 1 (solid magenta line) is a CACC-equipped vehicle following a speed reference; vehicle $i-1$ (solid cyan line) is the one that starts the platoon in the second position with an ACC as controller; and, vehicle i or follower is either an ACC-equipped vehicle (solid red line), a CACC-equipped vehicle (solid green line, considering that vehicle $i-1$ is always V2V-equipped) or an ACACC-equipped vehicle (solid blue line).

ACACC works as a classical CACC system while the communication with the preceding vehicle is available. Once the communication is lost, ACACC system significantly reduces speed oscillation introduced by the ACC-equipped vehicle, providing string stability but also increasing traffic flow by reducing inter-vehicle distances.

Finally, limits of the ACACC applications are tested. As already said, $5m/s$ is used as the maximum acceptable range for using ACACC. Specifically, Fig. 11 depicts the performance of the ACACC controller in comparison with ACC and CACC controllers when four ACC-equipped vehicles are between vehicle 1 and vehicle i . So, a string of six vehicles is considered. Speed difference between vehicle 1 and vehicle $i-1$ reach almost $5m/s$. V2V communication is only available between vehicle 1 and i . For notation, vehicle 1 (solid magenta line) is a CACC-equipped vehicle following a speed reference; vehicle $i-1$ (solid cyan line) is the one that starts the platoon in the fifth position with an ACC as controller; and, vehicle i or follower is either an ACC-equipped vehicle (solid red line), a CACC-equipped vehicle (solid green line, considering that vehicle $i-1$ is V2V-equipped) or an ACACC-equipped vehicle (solid blue line).

Even with 4 ACC-equipped vehicles without communications between leader and ego vehicles, ACACC preserves its ability to reduce speed oscillations and intervehicle-distance, improving consequently the traffic flow.

These simulations represent the closer behaviour to real traffic environment with a high penetration of ACC-equipped and CACC-equipped vehicles, giving an insight into the potential benefits of ACACC.

VI. EXPERIMENTAL RESULTS

Three cycabs were used as experimental vehicles. These vehicles are mobile platforms used in several research labs conceived for urban applications. From a kinematic point of view, cycabs can turn their rear wheels as a linear function of the steering angle of the front wheels [36]. The vehicle is controlled by a commanded velocity. The velocity is limited up to $4m/s$, because it is mainly designed for crowded areas where higher speeds can lead to unsafe situations. As ACACC has been designed for high-velocities, the proposed system is scaled to these low-speed platforms for having an experimental proof-of-the-concept.

The vehicle dynamic model for evaluating the performance of ACACC is presented in equation (20). Cycab real velocity responses have a characteristic overshoot preserved in the model.

$$G(s) = \frac{1}{0.8768s^2 + 1.252s + 1} \quad (20)$$

A. Control system stability

TABLE IV
CYCAB CACC PARAMETERS.

	K_{ext}^i	$k_{p,i}$	$k_{d,i}$	h_i
CACC _{STG}	K_{ext}^0	$k_{p,0} = 1.5$	$k_{d,0} = 0.2$	$h_0 = h_{CACC} = 0.6s$
CACC _{LTG}	K_{ext}^1	$k_{p,1} = 1.5$	$k_{d,1} = 0.2$	$h_1 = h_{ACC} = 1.5s$

TABLE V
CL POLES ($G/s, K_{ext}(\gamma)$). YK CONTROLLER RECONFIGURATION BETWEEN K_{ext}^0 AND K_{ext}^1 . CYCAB.

γ	CL poles
$\gamma = 0.0$	$[-6.28e^7, 0, -0.78 \pm 1.24]$
$\gamma = 0.1$	$[-6.28e^7, -6.28e^7, 0, 0, -0.78 \pm 1.24, -0.88 \pm 1.70i]$
$\gamma = 0.2$	$[-6.28e^7, -6.28e^7, 0, 0, -0.78 \pm 1.24, -0.88 \pm 1.70i]$
$\gamma = 0.3$	$[-6.28e^7, -6.28e^7, 0, 0, -0.78 \pm 1.24, -0.88 \pm 1.70i]$
$\gamma = 0.4$	$[-6.28e^7, -6.28e^7, 0, 0, -0.78 \pm 1.24, -0.88 \pm 1.70i]$
$\gamma = 0.5$	$[-6.28e^7, -6.28e^7, 0, 0, -0.78 \pm 1.24, -0.88 \pm 1.70i]$
$\gamma = 0.6$	$[-6.28e^7, -6.28e^7, 0, 0, -0.78 \pm 1.24, -0.88 \pm 1.70i]$
$\gamma = 0.7$	$[-6.28e^7, -6.28e^7, 0, 0, -0.78 \pm 1.24, -0.88 \pm 1.70i]$
$\gamma = 0.8$	$[-6.28e^7, -6.28e^7, 0, 0, -0.78 \pm 1.24, -0.88 \pm 1.70i]$
$\gamma = 0.9$	$[-6.28e^7, -6.28e^7, 0, 0, -0.78 \pm 1.24, -0.88 \pm 1.70i]$
$\gamma = 1.0$	$[-6.28e^7, 0, -0.88 \pm 1.70i]$

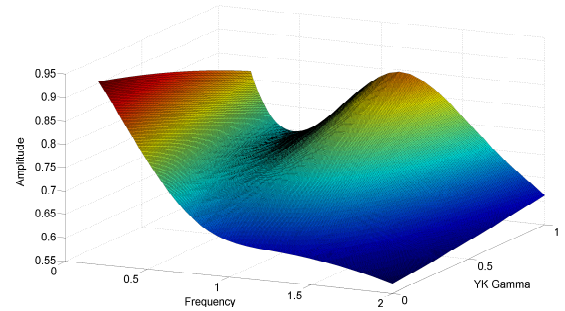


Fig. 12. String stability's surface for a Cycab depending on YK γ .

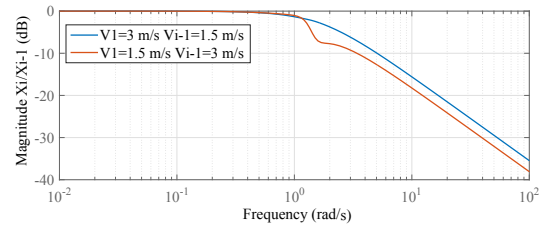


Fig. 13. String stability magnitude in dB for a cycab when communication with preceding vehicle is not available, but it is with the leader vehicle. $|V_1 - V_{i-1}^s| = 1.5m/s..$

Control system stability for the designed ACACC is studied in function of γ through equation (19). Controller gains in Table IV and model in equation (20) are considered in order

to obtain the CL poles shown in Table V. Control system stability is preserved for every value of γ .

String stability is analysed. When there is communication with the preceding vehicle, Fig. 12 represents the stability surface for ACACC in function of the γ value. Its infinity norm is always below the unity for any value of γ , proving string stability. On the other hand, when there is no communication with the preceding vehicle but with a leader in a string of three vehicles, the bode's diagram in Fig. 13 considers a difference between V_{i-1}^s and V_1 of $1.5m/s$ (a scale of 10 is considered in the YK gamma tuning for obtaining a low-velocity behaviour). String stability is again ensured even if communication with the preceding vehicle is not available.

B. Using IDM as preceding non V2V-equipped vehicle

The non V2V-equipped vehicle $i-1$ is a cycab with an IDM controller with the desired velocity of $33.33m/s$. As IDM controllers depend on the ego-velocity and the velocity of its preceding vehicle, both signals are scaled with a factor of 10 for obtaining a low-velocity behaviour. In the same way, the velocities used in the tuning of γ are scaled for proving the correct performance of the approach.

Figure 14 depicts the performance of the scaled ACACC controller in comparison with ACC and CACC controllers when an IDM-equipped cycab is the vehicle $i-1$. The top graph plots the velocity responses of the three cycabs in the string. The second depicts the different accelerations of these vehicles during the test. The third graph shows the relative distances to the preceding vehicle. And the bottom graph represents how γ is changed over time, together with the real time gap.

For notation, vehicle 1 (solid magenta line) is a cycab with a speed profile that goes from $1m/s$ to $3m/s$ or vice-versa with increasing steps of acceleration/deceleration; vehicle $i-1$ (solid cyan line) is the second cycab in the string with an IDM controller; and, vehicle i or follower in third position is either ACC (solid red line), CACC (solid green line) or ACACC (solid blue line).

The performance of the ACACC is well-proved. The hybrid behaviour between $CACC_{STG}$ and $CACC_{LTG}$ responses of the ACACC controller is preserved. Its response comes earlier when vehicle 1 is accelerating or braking. And the relative distance to vehicle $i-1$ is shorter than with the classical degradation to ACC, improving the capacity of the road.

Nevertheless, it is noteworthy to mention how at low-velocities the adapted time gap by the system is more sensitive to any velocity change, as well to the standstill distance. It explains why the variation of the real time gap time through γ becomes more complicated for the low-velocity test (see the bottom part in Fig. 14).

C. Using an ACC-equipped vehicle as preceding non V2V-equipped one

A scenario where vehicle $i-1$ is an ACC-equipped cycab is carried out. Please notice that the ACC shown here is string stable. The performance of the ACACC controller can

be accomplished with a stable ACC without endangering the experimental platforms.

Figure 15 depicts the performance of the ACACC controller compared to ACC and CACC when the non V2V-equipped vehicle is an ACC-equipped cycab. For notation, vehicle 1 (solid magenta line) is a cycab with the speed profile seen in the previous section; vehicle $i-1$ (solid cyan line) is the second cycab with an ACC controller; and vehicle i or follower in the third position is either ACC (solid red line), CACC (solid green line) or ACACC (solid blue line).

These low-speed tests demonstrate the good performance of the proposed system. ACACC controller responses faster to speed changes, while preserving better the string stability and improving the highway capacity with a shorter distance to vehicle $i-1$.

VII. CONCLUSIONS

This paper explores the benefit of using V2V-equipped vehicle information from a vehicle ahead in the string when the preceding vehicle is a non-equipped one to improve traffic flow. The proposed system provides string stable responses and, more interestingly, reduce inter-vehicle distances, providing tighter strings. System performance is evaluated using either a human driven vehicle (emulated by the IDM) or an ACC-equipped vehicle as preceding one.

The stable interpolation between CACC controllers with different time gaps is ensured thanks to the use of the YK parameterization. The string stability of the control structure is also demonstrated.

A comparative analysis using [11] models for ACC and CACC vehicles at high speeds and the IDM model as human driver vehicle is carried out. ACACC system exhibits a good performance, improving ACC response by providing a tighter string of vehicles, a faster response to speed changes and a better preservation of the string stability. These results are scaled to the low-velocity experimental platform for having an experimental proof-of-concept. The performance is well-proved, improving relative distance to the preceding vehicle and obtaining faster responses. Highway capacity improvement when using ACACC will be quantified and studied in function of the vehicles market penetration, to have a more fair comparison with results in [7] and [9].

Non-ideal V2V communication link needs to be studied in a future, analyzing the relationship between stability and delay. This would need another controller configuration that could be included into the YK parameterization. Additionally, when considering different braking capabilities in each of the vehicles in the string, a collision avoidance system is needed, which represents a different control system to be developed and included in the YK approach.

REFERENCES

- [1] ICCT. (2016) European vehicle market statistics.
- [2] E. Commission. (2012) Road transport. a change of gear.
- [3] G. Marsden, M. Mcdonals, and M. Bracktone., "Towards an understanding of adaptive cruise control," *Transportation Research Part C: Emerging Technologies*, vol. 9, no. 1, pp. 33–51, 2001.

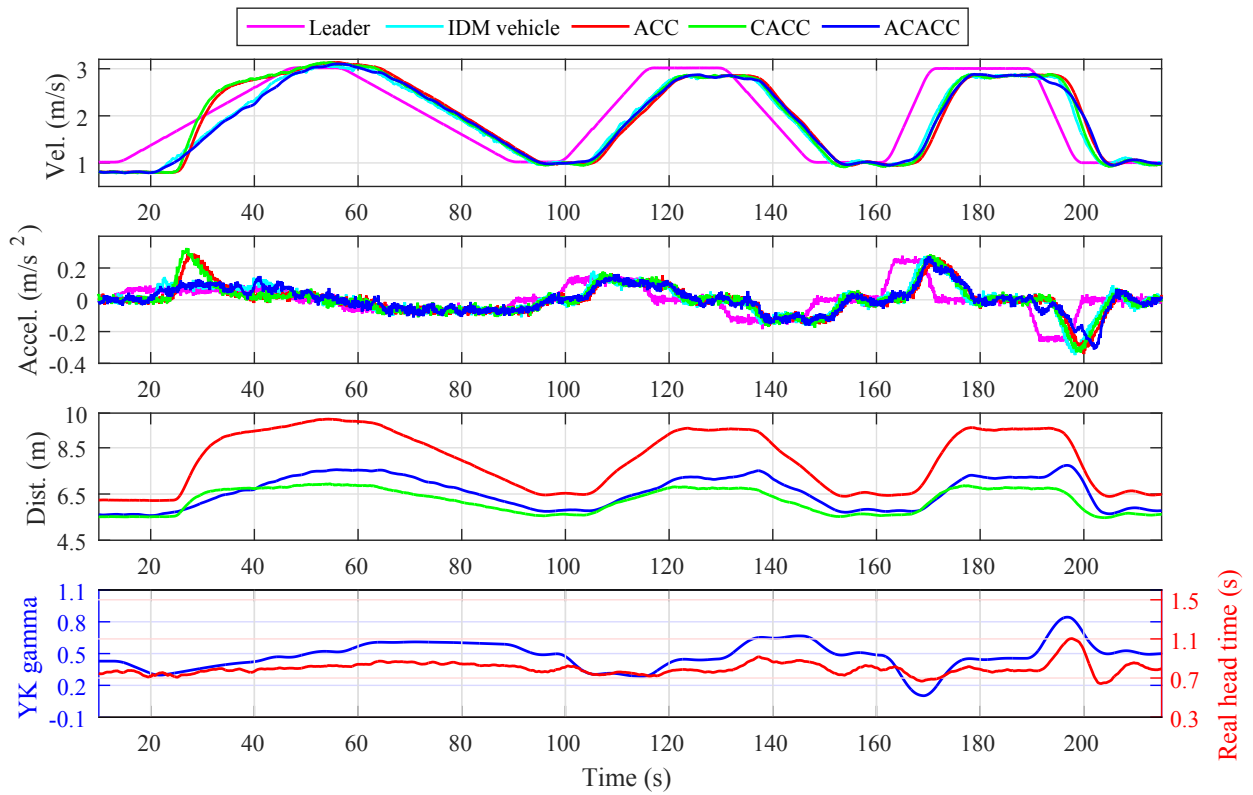


Fig. 14. Experimental results comparison among car-following policies using CACC, ACC and ACACC controllers when a non V2V-equipped cycab is in front. The non V2V-equipped is a cycab with an IDM with a desired velocity of 33.33m/s .

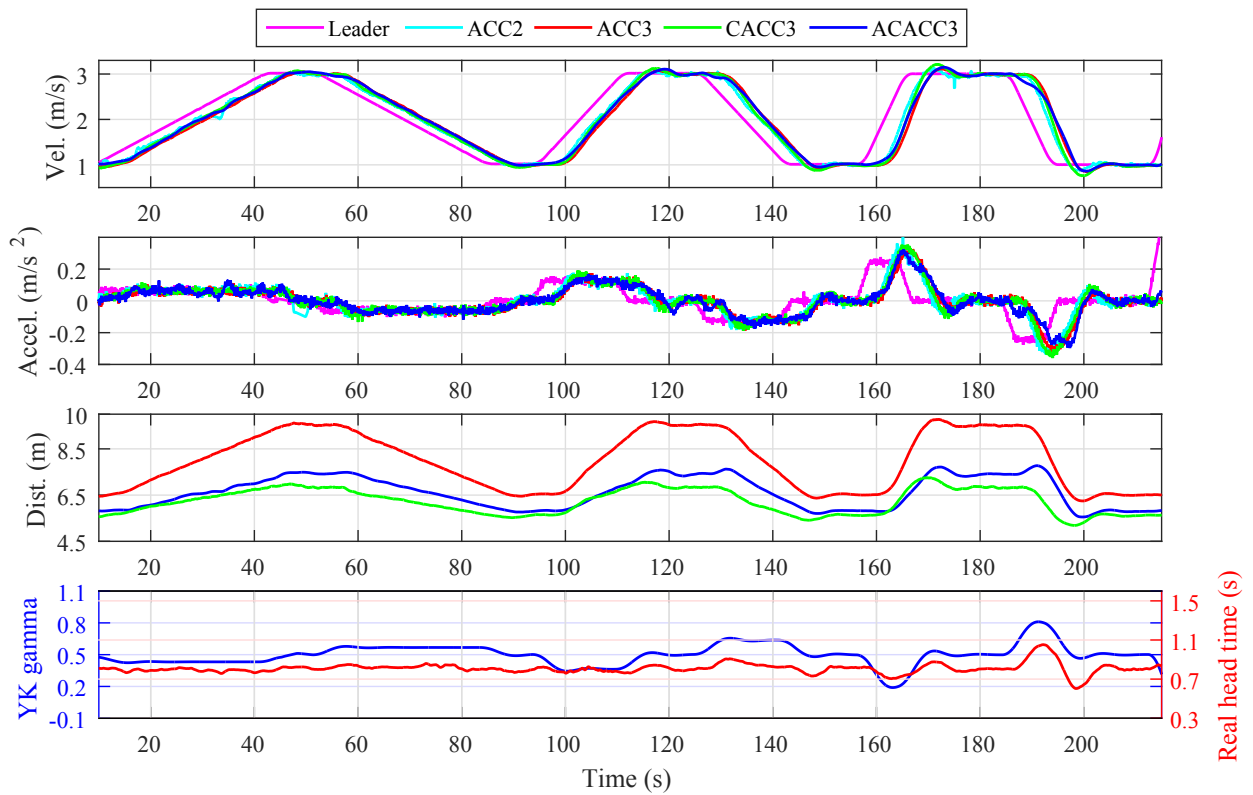


Fig. 15. Experimental results comparison among car-following policies using CACC, ACC and ACACC controllers when a non V2V-equipped cycab is in front. The non V2V-equipped is an ACC-equipped cycab.

- [4] J. Ploeg, B. T. Scheepers, E. van Nunen, N. van de Wouw, and H. Nijmeijer, "Design and experimental evaluation of cooperative adaptive cruise control," in *In 2011 14th International IEEE Conference on Intelligent Transportation Systems (ITSC)*, 2011, pp. 260–265.
- [5] A. Kesting, M. Treiber, M. Schnhof, and D. Helbing, "Adaptive cruise control design for active congestion avoidance," *Transportation Research Part C: Emerging Technologies*, vol. 16, no. 6, pp. 668–683, 2008.
- [6] A. Kesting, M. Treiber, and D. Helbing, "Extending adaptive cruise control to adaptive driving strategies," *Transportation Research Record: Journal of the Transportation Research Board.*, 2007.
- [7] S. Shladover, D. Su, and X. Y. Lu., "Impacts of cooperative adaptive cruise control on freeway traffic flow," *Transportation Research Record: Journal of the Transportation Research Board*, no. 2324, pp. 63–70, 2012.
- [8] C. Nowakowski, J. O'Connell, S. E. Shladover, and D. Cody, "Cooperative adaptive cruise control: Driver acceptance of following gap settings less than one second," in *Proceedings of the Human Factors and Ergonomics Society Annual Meeting*, vol. 54, no. 24. SAGE Publications Sage CA: Los Angeles, CA, 2010, pp. 2033–2037.
- [9] J. V. Werf, S. Shladover, M. Miller, and N. Kourjanskaia., "Effects of adaptive cruise control systems on highway traffic flow capacity," *Transportation Research Record: Journal of the Transportation Research Board*, no. 1800, pp. 78–84, 2002.
- [10] B. V. Arem, C. J. V. Driel, and R. Visser, "The impact of cooperative adaptive cruise control on traffic-flow characteristics," *IEEE Transactions on Intelligent Transportation Systems*, vol. 7, no. 4, pp. 429–436, 2006.
- [11] V. Milanés and S. E. Shladover, "Modeling cooperative and autonomous adaptive cruise control dynamic responses using experimental data," *Transportation Research Part C: Emerging Technologies*, vol. 48, pp. 285–300, 2014.
- [12] J. Ploeg, E. Semsar-Kazerooni, G. Lijster, N. van de Wouw, and H. Nijmeijer, "Graceful degradation of cacc performance subject to unreliable wireless communication," in *In 16th International IEEE Conference on Intelligent Transportation Systems*, 2013, pp. 1210–1216.
- [13] E. van Nunen, J. Verhaegh, E. Silvas, E. Semsar-Kazerooni, and N. van de Wouw, "Robust model predictive cooperative adaptive cruise control subject to v2v impairments," in *2017 IEEE 20th International Conference on Intelligent Transportation Systems (ITSC)*. IEEE, 2017, pp. 1–8.
- [14] G. Savaia, Z. A. Biron, and P. Pisu, "A receding horizon switching control resilient to communication failures for connected vehicles," in *ASME 2017 Dynamic Systems and Control Conference*. American Society of Mechanical Engineers, 2017, pp. V001T45A009–V001T45A009.
- [15] S. Gong, A. Zhou, J. Wang, T. Li, and S. Peeta, "Cooperative adaptive cruise control for a platoon of connected and autonomous vehicles considering dynamic information flow topology," *arXiv preprint arXiv:1807.02224*, 2018.
- [16] H. Niemann, J. Stoustrup, and R. B. Abrahamsen, "Switching between multivariable controllers," *Optimal control applications and methods*, vol. 25, no. 2, pp. 51–66, 2004.
- [17] S. a. Shahruz and S. Behtash, "Design of controllers for linear parameter-varying systems by the gain scheduling technique," *Journal of Mathematical Analysis and Applications*, vol. 168, no. 1, pp. 195–217, 1992.
- [18] D. J. Stilwell and W. J. Rugh, "Interpolation of observer state feedback controllers for gain scheduling," *IEEE transactions on automatic control*, vol. 44, no. 6, pp. 1225–1229, 1999.
- [19] —, "Stability preserving interpolation methods for the synthesis of gain scheduled controllers," *Automatica*, vol. 36, no. 5, pp. 665–671, 2000.
- [20] H. Niemann and J. Stoustrup, "An architecture for implementation of multivariable controllers," in *American Control Conference, 1999. Proceedings of the 1999*, vol. 6. IEEE, 1999, pp. 4029–4033.
- [21] J. P. Hespanha and A. S. Morse, "Switching between stabilizing controllers," *Automatica*, vol. 38, no. 11, pp. 1905–1917, 2002.
- [22] F. Blanchini, S. Miani, and F. Mesquine, "A separation principle for linear switching systems and parametrization of all stabilizing controllers," *IEEE Transactions on Automatic Control*, vol. 54, no. 2, pp. 279–292, 2009.
- [23] J. Stoustrup, "Plug & play control: Control technology towards new challenges," in *In European Control Conference*, 2009, pp. 1668–1683.
- [24] V. Milanés, S. Shladover, J. Spring, C. Nowakowski, H. Kawazoe, and M. Nakamura, "Cooperative adaptive cruise control in real traffic situations," *IEEE Transactions on Intelligent Transportation Systems*, vol. 15, no. 1, pp. 296–305, 2014.
- [25] F. Navas, V. Milans, and F. Nashashibi, "Using plug&play control for stable acc-cacc system transitions," in *In Intelligent Vehicles Symposium*, 2016.
- [26] G. J. Naus, R. P. Vugts, J. Ploeg, M. J. van de Molengraft, and M. Steinbuch, "String-stable cacc design and experimental validation: A frequency-domain approach," *IEEE Transactions on Vehicular Technology*, vol. 59, no. 9, pp. 4268–4279, 2010.
- [27] R. Rajamani, *Vehicle dynamics and control*, S. S. . B. Media., Ed., 2011.
- [28] L. Armstrong, "Dedicated short range communications (dsrc) home," 2002.
- [29] V. Kucera, "A method to teach the parameterization of all stabilizing controllers," *IFAC Proceedings Volumes*, vol. 44, no. 1, pp. 6355–6360, 2011.
- [30] K. Zhou, J. Doyle, and K. Glover., *Robust and Optimal Control*, P. Hall, Ed., 1996.
- [31] C. Nett, C. Jacobson, and M. Balas, "A connection between state-space and doubly coprime fractional representations," *IEEE Transactions on Automatic Control*, vol. 29, no. 9, pp. 831–832, 1984.
- [32] J. F. Pommaret and A. Quadrat, "Generalized bezout identity," in *Applicable Algebra in Engineering, Communication and Computing*, vol. 9, no. 2, 1998, pp. 91–116.
- [33] J. Y. Ishihara and R. M. Sales, "Doubly coprime factorizations related to any stabilizing controllers in state space," *Automatica*, vol. 35, no. 9, pp. 1573–1577, 1999.
- [34] F. Bu, H. S. Tan, and J. Huang, "Design and field testing of a cooperative adaptive cruise control system," in *In American Control Conference*, 2010, pp. 4616–4621.
- [35] A. Kesting, M. Treiber, and D. Helbing, "Enhanced intelligent driver model to access the impact of driving strategies on traffic capacity," *Philosophical Transactions of the Royal Society of London A: Mathematical, Physical and Engineering Sciences*, vol. 368, no. 1928, pp. 4585–4605, 2010.
- [36] S. Sekhavat and J. Hermosillo, "The cycab robot: a differentially flat system," in *IEEE/RS International Conference on Intelligent Robots and Systems*, 2000.